doi: 10.4149/gpb_2024029

Extremely low frequency pulsed magnetic field inhibits myocardial damage and apoptosis in rats with CLP-induced sepsis: A histopathological and immunohistochemical evaluation

Serkan Gürgül[1], Fikret Gevrek[2], Serkan Yelli[2], Fatma Betül Şeker[1] and Can Demirel[1]

[1] *Department of Biophysics, Faculty of Medicine, Gaziantep University, Gaziantep, Turkey*
[2] *Department of Histology and Embryology, Faculty of Medicine, Tokat Gaziosmanpasa University, Tokat, Turkey*

Abstract. We aimed to investigate whether pulsed magnetic fields (PMFs) (1 mT) may have preventive effects on myocardial damage and apoptosis in rats with sepsis. Twenty-eight adult Wistar albino rats were evenly distributed among four experimental groups, each consisting of seven rats: SH, LF-PMF, HF-PMF, and CLP. Sepsis induction was carried out *via* the cecal ligation and puncture (CLP) method, while rats in the LF-PMF and HF-PMF groups were exposed to 7.5 Hz and 15 Hz PMF, respectively, for duration of 24 hours. Following the removal of heart tissue, histological techniques were employed for the analysis. Histological scoring of apoptosis-related Bax, Bcl-2, and Acas-3 proteins as well as cTnI were performed in the heart tissue. The myocardial damage score significantly increased in the CLP group compared to the SH group ($p < 0.05$). Significant decreases were observed in Bcl-2 and cTnI protein levels in the CLP group, while significant increases were detected in the PMF groups ($p < 0.05$). An increase in Bax and Acas-3 protein levels, as well as the Bax/Bcl-2 ratio, was observed in the CLP group, with a decrease in the PMF groups ($p < 0.05$). The results demonstrate that PMF application has anti-apoptotic and therapeutic effects on septic heart tissue damage.

Key words: Apoptosis — Heart — Pulsed magnetic field (PMF) — Myocardial damage — Sepsis

Highlights

- PMF application prevents myocardial damage by suppressing sepsis-induced apoptotic cell death.
- PMF application suppresses immune expressions of pro-apoptotic Bax and Acas-3 proteins, while enhances anti-apoptotic Bcl-2 protein expression.
- PMF application exhibits its therapeutic effects on sepsis-induced myocardial damage by up-regulating cTnI protein expression in cardiac muscle.

Introduction

Sepsis is a systemic inflammation with a high morbidity and mortality rates attributed to a dysregulated host response to an infection (Yang et al. 2023). Multi-organ failure is one hallmark in patients with sepsis, and among the organs affected, the heart stands out (Zhang G et al. 2022). Myocardial dysfunction is one main cause of mortality in sepsis and is correlated with impaired circulation (e.g., microvascular dysfunction), depression (e.g., downregulated receptors and myocardial suppressants), inflammation, and cardiomyocyte apoptosis (Oberholzer et al. 2001a; Sun et al. 2011; Habimana et al. 2020; Zhang G et al. 2022).

Pathogen-targeting therapies with anti-inflammatory agents are essential for disease management; however,

Correspondence to: Serkan Gürgül, Department of Biophysics, Faculty of Medicine, Gaziantep University, TR-27310 Gaziantep, Turkey
E-mail: sgurgul@gantep.edu.tr

despite progress, there is a lack of sepsis-specific treatment (Vulczak et al. 2019). Therefore, developing new treatment strategies in sepsis management is an urgent need. Among others, pulsed magnetic field (PMF) is an innovative alternate therapy that modulates cellular signal pathways relevant to immunological and inflammatory functions in various cell types (Rosado et al. 2018). PMF applies intermittent, current pulse-generated magnetic field pulses over a short time frame, using a pulse repetition frequency (Waldorff et al. 2017). The effectiveness of PMF depends on factors such as waveform, intensity, and the pulse duration (Pieber et al. 2007). Since PMF is a non-invasive option without known side effects, it is used in medical fields like bone healing, skin lesion repair, and neo-angiogenesis with the FDA approval (van der Jagt et al. 2012, Bragin et al. 2018; Cadossi et al. 2020; Lee et al. 2022). Benefits of PMF exposure have been also shown in many medical conditions (Coskun et al. 2011; Comlekci et al. 2012; Markov et al. 2015; Capelli et al. 2017; Daish et al. 2018; Gessi et al. 2019; Mattsson et al. 2019; Flatscher et al. 2023).

Interventions aiming to modulate apoptosis have been reported to enhance survival in sepsis (Oberholzer et al. 2001b; Ayala et al. 2007; van der Poll et al. 2017). The reported therapeutic effects of PMF on apoptosis, oxidative stress, and oxidative stress-antioxidant defense mechanisms, alongside the well-established association between apoptosis and oxidative stress, make it a promising candidate as an alternate treatment strategy in sepsis management (Coskun et al. 2013; Vincenzi et al. 2017; Kannan and Jain 2020; Şimşek et al. 2022; Senol et al. 2023; Flatscher et al. 2023). Although PMF's therapeutic impact on the cardiovascular system exists (Soltani et al. 2023), detailed investigations at the molecular level are limited. Besides that, as far as we know, there is a lack of research focusing on the use of PMF for the treatment of sepsis-induced myocardial damage and apoptosis. Therefore, we aimed to explore the therapeutic effects of PMF on myocardial damage and apoptosis in cecal ligation and puncture (CLP) induced sepsis in rats by conducting histological and immunohistochemical analysis.

Material and Methods

Animals and experiment procedure

The study involved twenty-eight Wistar albino rats, aged 2.5 months and weighing 250 g, sourced from the Animal Experimentation Research Unit of Tokat Gaziosmanpaşa University (DETAB). Throughout the experiment, the rats were housed in standard polycarbonate plastic cages with sawdust beds, maintained on a 12-hour day-night cycle, in a stable environment at 20–22°C, and 50–60% relative humidity. They had free access to food and water.

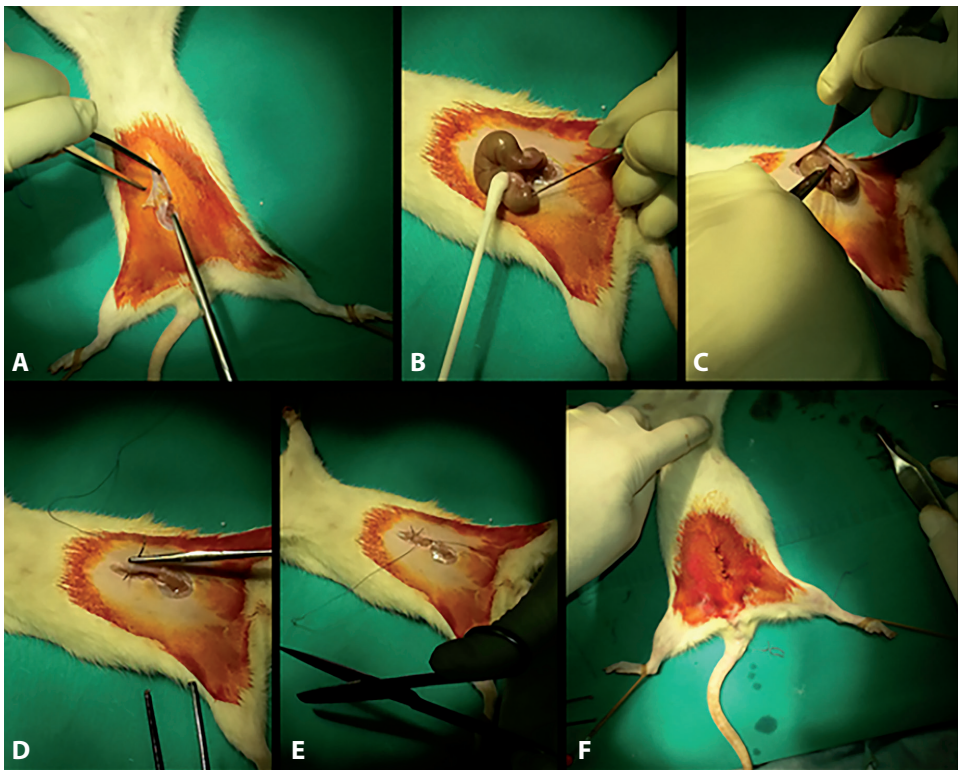

Figure 1. A. The subjects were immobilized on the operation table in the supine position and the abdominal skin was shaved totally, and laparotomy was carried out through a 3–4 cm midline incision. **B,C.** The cecum was isolated through laparotomy, and the ascending colon was gently touched downward to fill the cecum with feces. The cecum was ligated below the ileocecal valve using 3.0 silk thread, and the ventral side was perforated once using No.21-gauge needle to let fecal contents spread into the peritoneum. **D–F.** Then, the abdomen muscles and skin were closed with suture using 3.0 silk thread. Rats were resuscitated with normal saline (1 ml/100 g body weight given subcutaneously) at the end of the operation. In the sham group, the cecum was explored but CLP (cecal ligation and puncture) was not applied (Gevrek et al. 2023).

Upon approval of Decision No. 51879863-220 by the Tokat Gaziosmanpaşa University Animal Experiments Local Ethics Committee, the study was initiated. The rats were randomly allocated into four groups, each comprising seven rats:

1. Sham-operated group (SH): In this group of rats, an abdominal wall incision was made to visualize the cecum, and it was then re-inserted with no any intervention. Twenty-four hours later, after suturing, the rats were sacrificed.
2. Sepsis group (CLP): Rats in this group were underwent CLP procedure in order to induce sepsis experimentally. For this purpose, an abdominal wall incision was made to expose the cecum. Then, the lower part of the cecum was tied tightly with a thread, and some little feces was allowed to come out through a hole opened at the end of the cecum with a 2cc syringe needle, as seen in Figure 1. Five hours after sepsis was induced, the cecum went entirely black. So, the rats were made septic successfully. The rats in this group were kept in a Faraday cage within a plastic box for 24 h without PMF exposure.
3. Sepsis plus 7.5 Hz PMF exposure group (LF-PMF): After sepsis induction with the CLP method, rats in this group were housed in a Faraday cage within a plastic box and subjected to 7.5 Hz of 1 mT PMF treatment for 24 h.
4. Sepsis plus 15 Hz PMF exposure group (HF-PMF): After sepsis induction with the CLP method, rats in this group were subjected to 15 Hz of 1 mT PMF treatment for 24 h by the same route as the LF-PMF group.

All rats underwent CLP procedure were made septic successfully. At the termination, the rats were euthanized, and their hearts were extracted.

PMF exposure

In the study, a PMF system (ILFA Electronic Inc., Adana, Turkey) located in the Biophysics Department Laboratory of Tokat Gaziosmanpasa University Faculty of Medicine was used. The horizontal and uniform PMF was generated using a pair of Helmholtz coil (60 cm in diameter and 30 cm apart) housed in an earthed shielded Faraday cage (90×90×55 cm^3). Coils were constructed using electrically and thermally insulated copper wire with a diameter of 2.5 mm and 50 turns (Resistance: 0.78 Ω; Inductance: 8.8 mH) and were connected to a signal generator (ILFA Electronic Ltd.) to produce a magnetic field with a peak amplitude of 1 mT. The time-varying magnetic field adopted a quasi-triangular waveform with a rise time of 0.3 ms and a fall time of 9.7 ms, as previously described by Gul et al. (2018).

PMF exposure commenced five hours after sepsis induction, with the rats placed inside plastic boxes (26×17×13 cm^3) positioned at the center of the coils. Prior to the PMF application, the accuracy of the experimental setup, along with the homogeneity of the PMF (determined as 95% within plastic box), was verified. The ambient magnetic field (50 μT) and the peak amplitude of magnetic field (1 mT) generated by the coils were measured using a Tesla meter equipped with a Hall-effect probe (Sypris 6010; F.W. Bell, CA, USA). The corresponding induced peak electrical field value within the plastic box, positioned between the Helmholtz coils, was 0.24–0.27 V/m, calculated based on Faraday's law (Mert et al. 2010; Gul et al. 2018). The PMF application was conducted within a quiet room for 24 hours. Two distinct pulses were used: one with a frequency of 7.5 Hz (LF-PMF group), and the other with a frequency of 15 Hz (HF-PMF group). The magnetic flux density for both pulses was maintained at 1 mT. Throughout the experiment, the room temperature (22–24°C) and relative humidity (50–60%) were monitored. During experiments, no considerable temperature changes between two activated coils were detected. In terms of human health, the European Union and the International Commission on Non-Ionizing Radiation Protection (ICNIRP) have suggested lower safety thresholds for general public, whereas the American Industrial Hygiene Association (AIHA) and the American Conference of Governmental Industrial Hygienists (ACGIH) have endorsed an upper safety limit of 1mT magnetic field intensity for occupational exposure. Together with that, in various studies, 7.5 Hz and 15 Hz of 1 mT PMFs applications have promoted cell proliferation and differentiation, as well as tissue healing and bone mass enhancement (Chang et al. 2006; Zhai et al. 2016; Wang et al. 2017); therefore, we administered these two different frequencies of PMF at 1 mT magnetic flux density (Gevrek et al. 2023).

Histological analyzes

Heart samples were fixed in 4% buffered neutral formalin for 72 h, followed by a 12-h wash under running tap water. Dehydrated through ascending alcohol series from 70% to absolute, cleared in xylene series, and embedded in paraffin blocks at 60°C. Serial sections, 5 μm in thickness, were then cut from the heart samples embedded in the paraffin blocks using a rotary microtome (Leica RM2135, Wetzlar, Germany). Tissue sections were taken on lams covered Poly-L-Lysine and stained according to hematoxylin-eosin and immunohistochemical staining protocols.

Hematoxylin-eosin staining

Formalin-fixed paraffin-embedded heart tissue sections were deparaffinized in xylenes (3×5 min) and rehydrated in descending alcohol series (from 100 to 70%) and distilled water, then incubated in hematoxylin for 10 min. After being washed with running tap water for 5 min, dipped in acid alcohol, and put in distilled water, the slides were incubated

in eosin solution. The sections were immersed in distilled water to remove excess dye, dipped in 80% alcohol, and left in 90, 96, and 100% alcohol series for 2, 3, and 5 min, respectively. They were cleared in xylene (3×10 min) and mounted under a coverslip. After drying, the sections were analyzed histologically through a light microscope.

Myocardial damage analyzes were performed on 10 sections of each animal and an average of 20–25 areas in each section using a computer-assisted light microscope (Nikon Eclipse 200 Serial No: T1al 944909, Japan) image with a camera integrated into the microscope (Nikon Ds-Fi1, Japan). It was transferred to the monitor and performed with the help of the NIS-Element program. Microscopic analyzes were carried out in a blinded manner by the researcher who was not aware of the working groups based on the coding system. In order to numerically express the degree of histological damage, the organization pattern and degeneration of muscle fibers were graded (Erkanli et al. 2005). The categorical scoring system utilized for assessing cardiac muscle fiber organization is as follows: "0" score indicates normal heart muscle tissue, exhibiting an intact and organized structure, "1" score represents slightly damaged heart muscle tissue, displaying initial signs of disorganization, "2" score reflects moderately damaged and disorganized heart muscle tissue, showing a notable level of structural disruption, and "3" score indicates severely disorganized cardiac muscle tissue with impaired transverse and intercalated disc striations. The muscle fibers were counted categorically according to this scoring system, and the degrees of myocardial damage were defined. The results were converted into weighted myocardial damage scores using the formula below, where i is the categorical degree of the muscle damage regarding scoring system. Then, the mean weighted myocardial damage scores of the groups were calculated and compared statistically.

$$Weighted\ myocardial\ damage\ score = \\ = \frac{\sum_{i=0}^{n=3}[(Damage\ Score)_i \times (i)]}{\sum_{i=0}^{n=3}(Damage\ Score)_i}$$

Immunohistochemistry

An indirect immunohistochemistry protocol for formalin fixed paraffin embedded rat tissues was conducted on the heart sample sections to detect immune expression of some apoptosis pathway molecules (Bax, Bcl-2, and Acas-3 (caspase-3)) and cardiac isoform of Troponin-I (cTnI). In brief, heart tissue sections were mounted on slides, deparaffinized in etuve at 60°C and xylene series and rehydrated through descending alcohols (from absolute to 70% and distilled H_2O). After antigen retrieval with citric acid (10 mM), the sections were incubated in 3% hydrogen peroxide (H_2O_2) to quench endogenous peroxidase activity washed in phosphate buffer solution (PBS) (3×5 min) and encircled by a pap pen (hydrophobic pen). The slides were incubated in 1% bovine serum albumin (BSA) for 15 min to block them. Removed the BSA without washing, and the slides were incubated with primary antibodies to Acas-3, Bax, and Bcl-2 (1:50, Santa Cruz) and cTnI (1:100) at 4°C in a humidified and dark environment overnight. After washing with PBS (3×5 min), the samples were incubated with a biotinylated secondary antibody (Vector Laboratories, USA) for 45 min at room temperature in a dark, humidified environment. Subsequently, they underwent a PBS wash (3×5 min) and were incubated with an HRP-labeled streptavidin secondary antibody (GE Healthcare, UK) for an additional 30 min at room temperature. Samples were incubated with amino ethyl carbazole (AEC, ScyTek Laboratories Inc.) chromogen after washing with PBS (3×5 min) to visualize immunoreactivity. Sections were counterstained with hematoxylin and were mounted under a coverslip in an aqueous mounting reagent (Invitrogen, Carlsbad, CA) after washing in distilled water. In some slides, PBS was dropped onto the sections instead of a primary antibody for the negative control, and no immunostaining was observed. Randomly selected five areas in each section were analyzed under the light microscope at 400× magnification (Nikon Eclipse E200) using the NIS-Elements software program (Hasp ID: 6648AA61; Nikon) to define the immune-stained cells. The staining intensity of the molecules was assessed using a four-level categorical scoring system to determine their immune expression levels. The criteria for the immunostaining scoring system are as follows: "0+" score indicates no staining, "1+" score indicates weak but detectable staining, "2+" score indicates moderate staining, and "3+" score indicates strong/intense staining (Gevrek et al. 2024). The cells were counted categorically according to these criteria, and immunostaining intensities were defined. The results were converted into H-score values, a semiquantitative evaluation system of immunohistochemistry, using the formula $[\Sigma Pi \times (i + 1)]$. In this formula, i is the staining intensity score, and Pi is the percentage of stained cells. The mean immunostaining H-scores of the groups were accounted for and compared statistically.

Statistical analysis

After checking with Shapiro-Wilks test to determine whether the data was normally distributed, data were analyzed using Kruskal Wallis-H test followed by Bonferroni adjustment for multiple comparisons. If the p value is < 0.05, it was considered statistically significant. All statistical analyzes were conducted using SPSS for Windows (Release-20.0.0, IBM Co., Somers, NY, US) and Statistica 8.0 Program (StatSoft Inc., OK, USA), whenever applicable. Data were expressed as the mean ± SD.

Results

Histopathologic results

In the histopathologic examination, a notable increase in the myocardial damage score was evident in the CLP group compared to the SH group, reaching statistical significance ($p < 0.05$, $n = 7$, $X^2 = 7.87$, df = 3) (Fig. 2). Throughout the microscopic analysis, we observed a typical histological structure in the heart tissue of the SH group rats (Fig. 3A). However, the CLP group exhibited extensive histological damages, including disorganized muscle tissue and structural disruption, hemorrhagic and necrotic areas, inflammatory cell infiltration, apoptotic cells with pyknotic nuclei, and regions with pale staining (Fig. 3D). The analyzes also showed a decrease in histopathological injuries in both groups of PMF, where both PMF groups had almost similar appearances to each other (Fig. 3B,C).

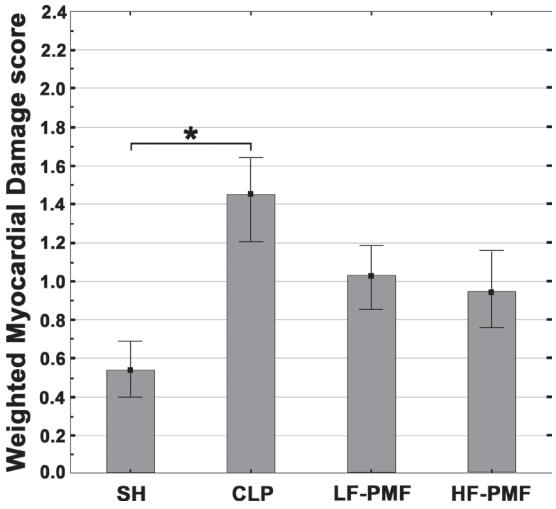

Figure 2. Weighted myocardial damage scores of the groups. Data are means ± SD. Kruskal-Wallis-H test followed by Bonferroni adjustment for multiple comparisons were used. * $p < 0.05$ *vs.* SH group, $N_{Total} = 28$ ($n = 7$ for each group), $X^2 = 7.87$, df = 3. SH, sham-operated group; CLP, sepsis-induced group; LF-PMF, CLP (Sepsis) + 1 mT 7.5 Hz PMF-treated group; HF-PMF, CLP (Sepsis) + 1 mT 15 Hz PMF-treated group. PMF, pulsed magnetic field.

Immunohistochemical results

The immunohistochemical analysis revealed changes in immune expression of crucial protein markers linked to myocardial apoptosis and injury. Specifically, the Bcl-2 protein H-score values were significantly reduced in the CLP group compared to the SH group ($p < 0.001$, $n = 7$, $X^2 = 16.58$, df = 3), indicative of decreased anti-apoptotic activity in myocardial tissue following CLP-induced sepsis (Figs. 4A and 5). Remarkably, both LF-PMF and HF-PMF therapies led to a significant elevation in Bcl-2 H-score values compared to the CLP group ($p < 0.001$ *vs.* LF-PMF and HF-PMF, $n =$

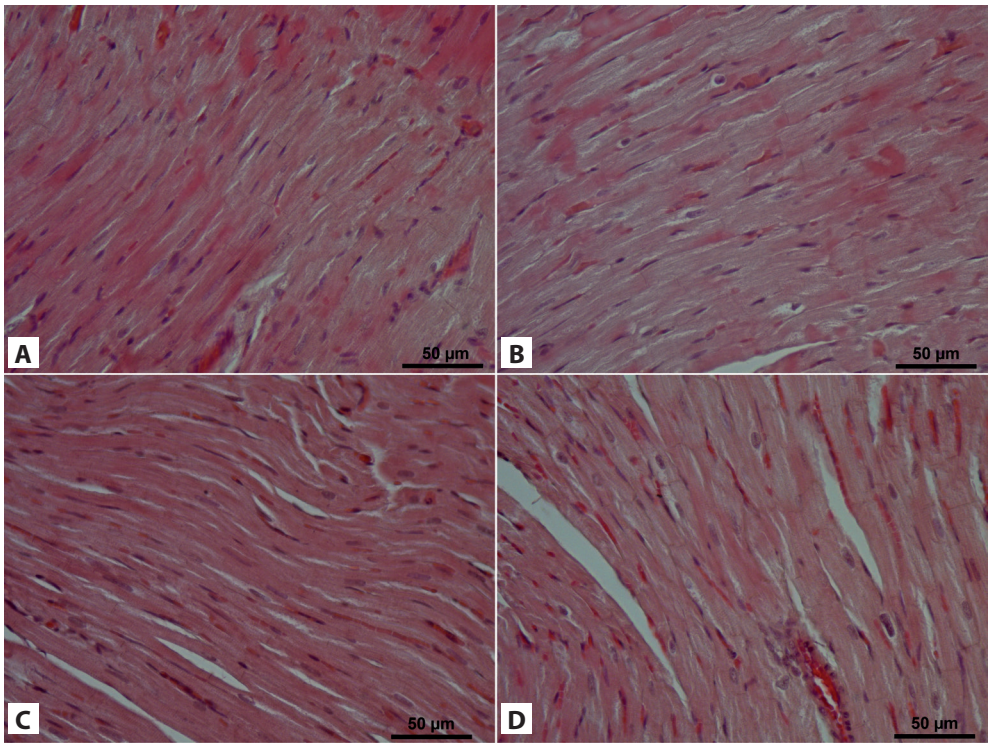

Figure 3. Representative microscopic images showing hematoxylin-eosin-stained cross-sections of the rat heart tissues within the groups: SH (**A**), LF-PMF (**B**), HF-PMF (**C**), CLP (Sepsis, **D**). Bar: 50 µm. SH exhibits the characteristic histological structure of heart tissue. LF-PMF and HF-PMF have moderate tissue damage, whereas CLP (Sepsis) has severe tissue damage. For abbreviations, see Figure 2.

7, X^2 = 16.58, df = 3), underscoring the potential of PMF in mitigating apoptosis (Figs. 4A and 5).

Conversely, immune expression of pro-apoptotic pathways demonstrated an opposing trend. The Bax H-score, Bax/Bcl-2 ratio, and Acas-3 H-score exhibited significant increases in the CLP group compared to the SH group (p < 0.01 for Bax, p < 0.001 for Bax/Bcl-2 ratio and Acas-3, n = 7, X^2 = 12.01 for Bax, X^2 = 14.73 for Bax/Bcl-2 ratio, X^2 = 14.05 for Acas-3, df = 3), indicative of heightened apoptotic activity in septic myocardial tissue (Figs. 4B–D and 5). However, both LF-PMF and HF-PMF therapies resulted in notable reductions in the immune expression of Bax H-score, Bax/Bcl-2 ratio, and Acas-3 when compared to the CLP group (p < 0.01 *vs.* LF-PMF and HF-PMF for Bax, p < 0.001 *vs.* LF-PMF and HF-PMF for Bax/Bcl-2 ratio and Acas-3, n = 7, X^2 = 12.01 for Bax, X^2 = 14.73 for Bax/Bcl-2 ratio, X^2 = 14.05 for Acas-3, df = 3), suggesting the potential of PMF in attenuating pro-apoptotic signaling pathways (Figs. 4B–D and 5).

Furthermore, the cTnI, a crucial marker of myocardial injury, exhibited a significant decrease in the CLP group compared to the SH group (p < 0.001, n = 7, X^2 = 14.87, df = 3), indicating sepsis-induced myocardial damage (Figs. 6 and 7A,D). Interestingly, both LF-PMF and HF-PMF therapies led to significant increases in cTnI immune expression compared to the CLP group (p < 0.05 *vs.* LF-PMF, p < 0.001 *vs.* HF-PMF, n = 7, X^2 = 14.87, df = 3), implying a potential

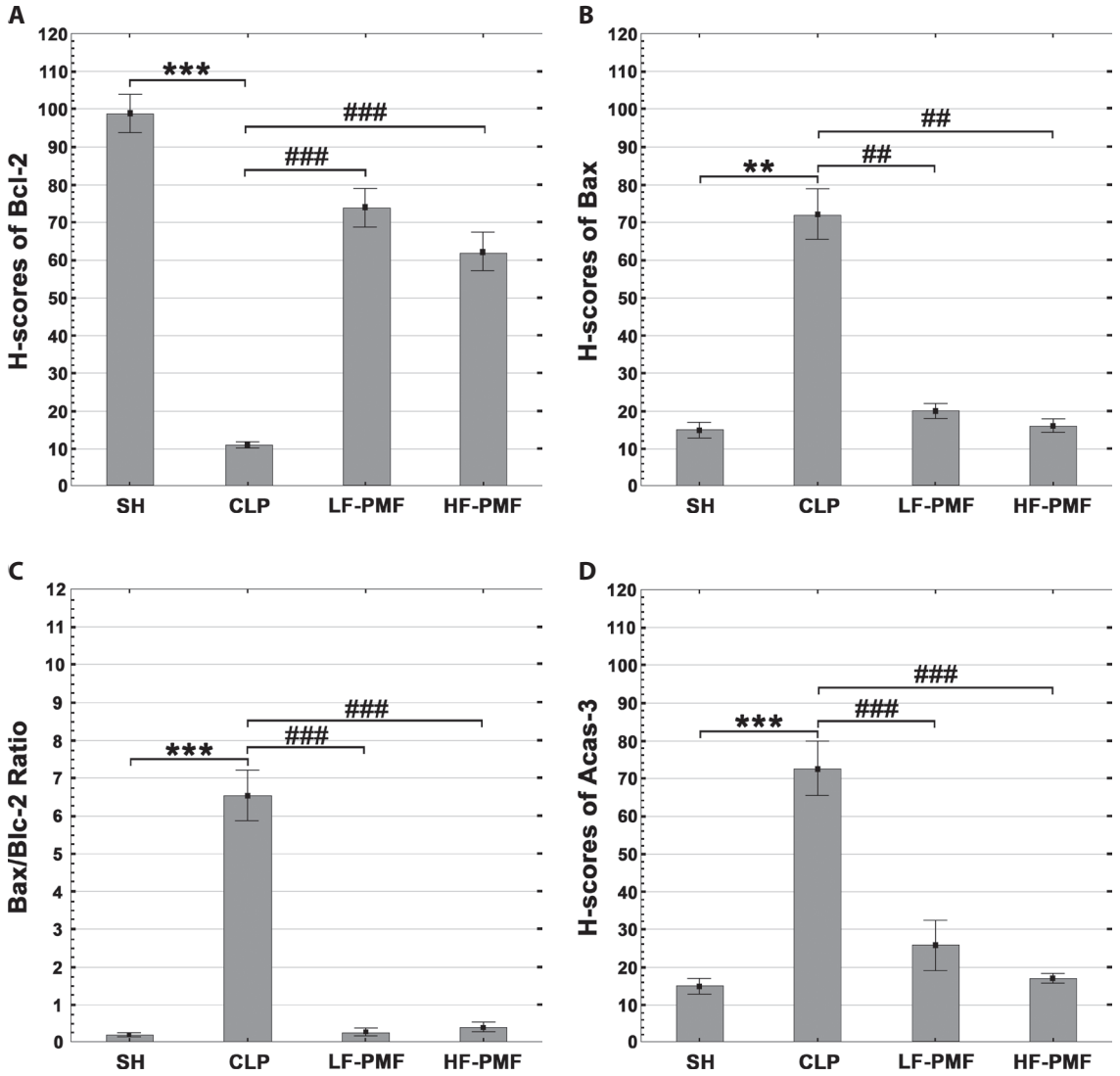

Figure 4. Immunohistochemical staining intensity scores (H-scores) of Bcl-2 (**A**), Bax (**B**), Bax/Bcl-2 ratio (**C**) and Acas-3 (**D**) in the groups. Data are means ± SD. Kruskal-Wallis-H test followed by Bonferroni adjustment for multiple comparisons were used. ** p < 0.01 and *** p < 0.001 *vs.* SH group, ## p < 0.01 and ### p < 0.001 *vs.* CLP group, N_{Total} = 28 (n = 7 for each group), X^2 = 16.58 for Bcl-2, X^2 = 12.01 for Bax, X^2 = 14.73 for Bax/Bcl-2 ratio, X^2 = 14.05 for Acas-3, df = 3. For abbreviations, see Figure 2.

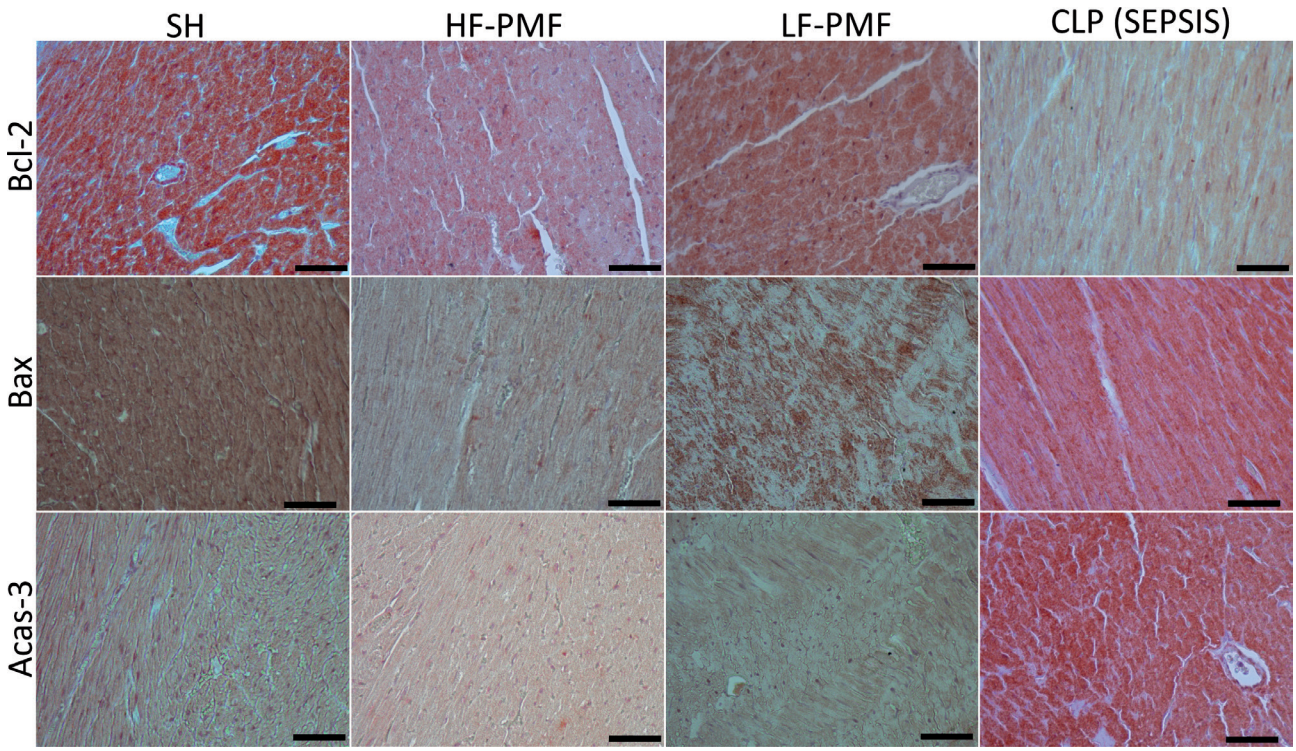

Figure 5. A representative photomicrograph of immune staining of the apoptotic (Acas-3, Bax) and antiapoptotic (Bcl-2) proteins are shown in the cardiac muscle tissues of the groups. Immune expressions of Acas-3 and Bax are greater in CLP than in other groups. Notable reductions are observed in the LF-PMF and HF-PMF groups *versus* CLP. Bcl-2's immune expression exhibits *vice versa* appearance with that of Acas-3 and Bax. Bar: 50 μm. For abbreviations, see Figure 2.

protective effect of PMF against sepsis-induced myocardial injury (Figs. 6 and 7B–D).

Discussion

In our study, significant changes were observed in related for apoptosis Bcl-2, Bax, and Acas-3 (caspase-3) proteins as well as cTnI protein and Bax/Bcl-2 ratio in the CLP and PMF groups. These changes are strong evidence that sepsis causes damage and apoptosis in myocardial cells and that PMF treatment has preventive effects on this damage.

Apoptosis is a meticulously regulated, energy-dependent suicide program in which a cell initiates a signaling cascade resulting in cell death without eliciting an inflammatory response (Gustafsson et al. 2007). The Bcl-2/Bax/Cleaved caspase-3 apoptotic signaling pathways, as a signal pathway regulating cell apoptosis and survival, play a significant role in various diseases, including many cardiac diseases (Thornberry and Lazebnik 1998). Bcl-2 is a key anti-apoptotic protein, and high expression levels indicate inhibition of apoptotic death (Ellis et al. 1991; Oltvai et al. 1993; Cory and Adams 1998). Bax, identified through immunoprecipitation along with Bcl-2, is the foremost pro-apoptotic homolog. Accelerated apoptotic death occurs when Bax is overexpressed in cells (Haddad et al. 2007; Qin et al. 2008). It has been demonstrated that Bax forms heterodimers with Bcl-2, thereby mitigating the impact of Bcl-2 on cellular survival (Oltvai et al. 1993). When the Bcl-2/Bax ratio increases, apoptosis is inhibited, and when the ratio decreases, apoptosis is promoted (Qin et al. 2008). Caspase-3, a member of the caspase family, plays a central role in the execution of apoptosis (Porter et al. 1999). Apoptosis is accelerated with high caspase-3 expression (Pu et al. 2017). It is well-established that proteins from the Bcl-2 family and caspase family play a central role in regulating apoptosis in the cardiovascular system (Kirshenbaum et al. 1997; Kang et al. 2000; Zhu et al. 2001; Radhakrishnan et al. 2009). The role of apoptosis in the cardiovascular system is crucial, particularly in the development of cardiac pathologies such as heart diseases (Bennett 2002). An increase or dysregulation of apoptosis can lead to myocardial damage and sepsis triggers myocardial apoptosis (Krijnen et al. 2002). Based on the provided information and existing literature, reductions observed in the Bcl-2 expression level and the increases in the Bax, the Acas-3, and the Bax/Bcl-2 ratio in the CLP group relative to SH can be inter-

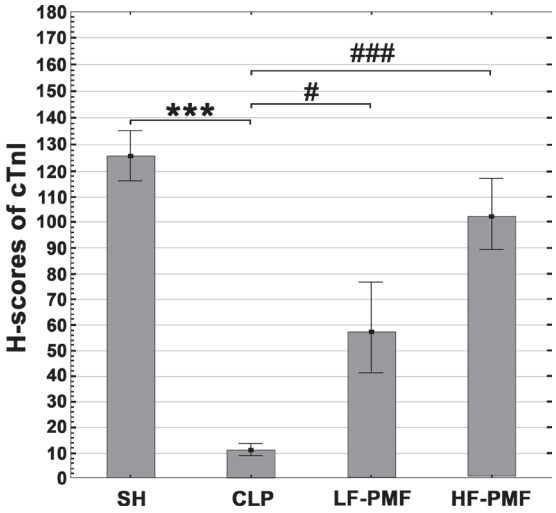

Figure 6. Immunohistochemical staining intensity H-scores of cTnI by the groups. Data are means ± SD. Kruskal-Wallis-H test followed by Bonferroni adjustment for multiple comparisons were used. *** $p < 0.001$ *vs.* SH group, # $p < 0.05$ and ### $p < 0.001$ *vs.* CLP group, $N_{Total} = 28$ ($n = 7$ for each group), $X^2 = 14.87$, df = 3. For abbreviations, see Figure 2.

preted as the sepsis induces myocardial apoptosis, and, thus, myocardial damage (Figs. 4A–D and 5). On the other hand, cTnI is one of three contractile regulatory troponin proteins responsible for regulating calcium-mediated interactions between actin and myosin myofilaments in cardiac muscles (Babuin et al. 2005). It is accepted as a sensitive biomarker of myocardial damage (Mair 1997; Negahdary et al. 2016; Wang et al. 2020) and the loss of cTnI immunoreactivity in myocardial cells indicates a pronounced extent of degeneration and necrosis (Tunca et al. 2009). Therefore, relative to the SH group, the reduction observed in the expression level of cTnI protein in the CLP strongly support our suggestion, indicating that sepsis induces myocardial damage (Figs. 6 and 7A,D). In this context, our results are consistent with the literature. Results from the histopathological evaluations where extensive histological damages were observed provide further evidence for the findings (Fig. 3A,D), whereas also being consistent with the previous reports (Zhang R et al. 2022; Zhao and Cheng 2022). The overall results reveal that sepsis was induced in the rats following their exposure to CLP in our experimental setup.

While studies on PMF therapy in sepsis treatment are limited, it has been demonstrated that in inflammatory diseases, PMF can propagate throughout the entire signal transduction pathway and significantly amplify, thus altering cell behavior (Ross et al. 2017). *In vitro* studies have shown that PMF treatment with different frequencies and wavelengths induces apoptosis in cancerous cells and alters apoptosis-related proteins (Amiri et al. 2018). Lee et al. (2022) recently performed a study to examine the potential alleviating effects of PMF (75 Hz, 14.67 mT, for up to 5 days) on bacterial sepsis in a murine model of lipopolysaccharide (LPS)-induced

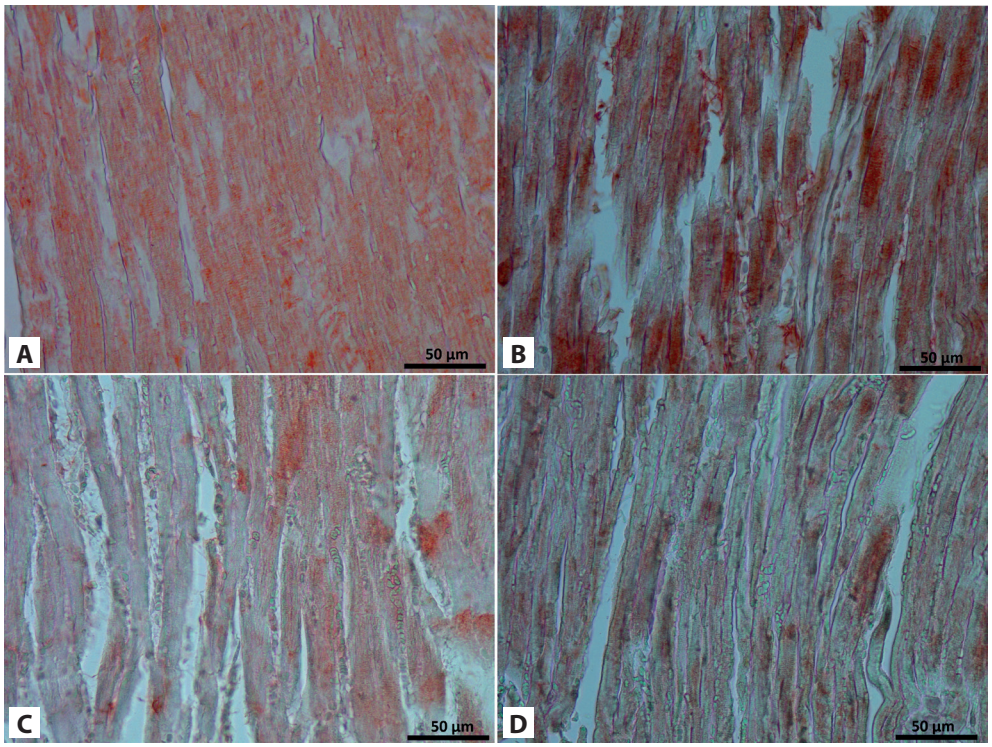

Figure 7. A representative image of cTnI immunohistochemical staining of the groups: SH (**A**), HF-PMF (**B**), LF-PMF (**C**) and CLP (**D**). The CLP group exhibits a significantly weaker staining intensity compared to the others. Notable improvements are observed in the LF-PMF and HF-PMF groups *versus* CLP. Bar: 50 µm. For abbreviations, see Figure 2.

septic shock. The study showed the exposure to PMF led to a reduction in septic shock-related mortality and prevented LPS-induced multiple organ failure multiple organ failure, including lung, liver, kidneys and spleen, in mice through the suppression of systemic immune and inflammatory responses (Lee et al. 2022). Previously, we conducted a study to explore the potential effects of 1 mT PMF (7.5 Hz and 15 Hz, for 24 h) on septic liver tissue injury triggered by CLP in rats. In the study, we observed that the exposure to 1 mT PMF reduced immune expression levels of Bax, Acas-3, and hypoxia-inducible factor (HIF)-1α (a factor involved in hypoxia induced apoptosis), increased Bcl-2 expression, and alleviated sepsis-related liver damage in rats (Gevrek et al. 2023). In the current study, the increases observed in the Bcl-2 expression levels and the reductions in the Bax, Acas-3, and the Bax/Bcl-2 ratios in both PMF groups relative to the CLP are evidenced that PMF prevents sepsis-induced myocardial apoptosis and, thus, myocardial damage (Figs. 4A–D and 5). The significant increases in myocardial cTnI expression levels observed in both PMF groups relative to the CLP strongly support our suggestion, indicating that PMF prevents sepsis-induced myocardial damage (Figs. 6 and 7B–D). Results from the histopathological evaluations where notable improvements were observed provide further evidence for the findings (Fig. 3B–D).

In conclusion, the application of PMF at a magnetic field intensity of 1 mT and at different frequencies (7.5 Hz and 15 Hz) to the rats with septic myocardial damage prevents apoptotic cell death through up-regulating anti-apoptotic pathway molecule Bcl-2 expression, and by down-regulating apoptotic pathway molecules Acas-3 and Bax expressions. Besides that, exposure to PMF also up-regulates cTnI, a sensitive biomarker of myocardial damage. Thus, it can be said that PMF has the potential to prevent apoptotic cell death and myocardial damage in septic myocardium. To our knowledge, the present study stands out as one of a kind, unveiling the therapeutic effects of PMF (7.5 Hz and 15 Hz, 1 mT; for 24 h) against sepsis-related myocardial damage. Our study, along with the histopathological examinations, provides crucial information regarding changes in the immunoreactivity of apoptotic-antiapoptotic markers (Bcl-2, Bax and Acas-3) and cTnI following PMF exposure in septic rat myocardium. Sepsis is a widespread cause of myocardial damage, observed in a significant portion of sepsis patients (Cheadle et al. 1996; Esper and Martin 2009). Preventing myocardial apoptosis may help impede the onset and progression of cardiovascular diseases. These findings would establish a crucial foundation for future research and clinical studies aimed at developing innovative strategies for the treatment of cardiovascular health issues arising from sepsis.

Conflicts of interest. The authors declare no competing interests.

Acknowledgements. We would like to thank Prof. Nurşah Başol for her kind support in establishing basic laboratory infrastructure.

Author contributions. SG, CD, and FG contributed to the study design. SG and SY conducted the murine model of sepsis. SG, FG and SY were involved in collecting and analyzing the data. FBŞ assisted with the literature review. All authors contributed to interpret the data for the work. SG wrote and drafted the manuscript.

References

Amiri M, Basiri M, Eskandary H, Akbarnejad Z, Esmaeeli M, Masoumi-Ardakani Y, Ahmadi-Zeidabadi M (2018): Cytotoxicity of carboplatin on human glioblastoma cells is reduced by the concomitant exposure to an extremely low-frequency electromagnetic field (50 Hz, 70 G). Electromagn. Biol. Med. **37,** 138-145 https://doi.org/10.1080/15368378.2018.1477052

Ayala A, Wesche-Soldato DE, Perl M, Lomas-Neira JL, Swan R, Chung CS (2007): Blockade of apoptosis as a rational therapeutic strategy for the treatment of sepsis. Novartis Found. Symp. **280,** 37-164 https://doi.org/10.1002/9780470059593.ch4

Babuin L, Jaffe AS (2005): Troponin: the biomarker of choice for the detection of cardiac injury. CMAJ **173,** 1191-1202 https://doi.org/10.1503/cmaj/051291

Bennett MR (2002): Apoptosis in the cardiovascular system. Heart **87,** 480-487 https://doi.org/10.1136/heart.87.5.480

Bragin DE, Bragina OA, Hagberg S, Nemoto EM (2018): Pulsed electromagnetic field (PEMF) mitigates high intracranial pressure (ICP) induced microvascular shunting (MVS) in rats. Acta Neurochir. Suppl. **126,** 93-95 https://doi.org/10.1007/978-3-319-65798-1_20

Cadossi R, Massari L, Racine-Avila J, Aaron RK (2020): Pulsed electromagnetic field stimulation of bone healing and joint preservation: Cellular mechanisms of skeletal response. J. Am. Acad. Orthop. Surg. Glob. Res. Rev. **4,** e1900155 https://doi.org/10.5435/JAAOSGlobal-D-19-00155

Capelli E, Torrisi F, Venturini L, Granato M, Fassina L, Lupo GFD, Ricevuti G (2017): Low-frequency pulsed electromagnetic field is able to modulate miRNAs in an experimental cell model of Alzheimer's disease. J. Healthc. Eng. **2017,** 1-10 https://doi.org/10.1155/2017/2530270

Chang K, Chang WH, Tsai MT, Shih C (2006): Pulsed electromagnetic fields accelerate apoptotic rate in osteoclasts. Connec. Tissue Res. **47,** 222-228 https://doi.org/10.1080/03008200600858783

Cheadle WG, Mercer-Jones M, Heinzelmann M, Polk HC Jr (1996): Sepsis and septic complications in the surgical patient: who is at risk? Shock **6,** S6-S9 https://doi.org/10.1097/00024382-199610001-00003

Comlekci S, Coskun O (2012): Influence of 50 Hz-1 mT magnetic field on human median nerve. Electromagn. Biol. Med. **31,** 285-292 https://doi.org/10.3109/15368378.2012.662190

Cory S, Adams JM (1998): Matters of life and death: programmed cell death at Cold Spring Harbor. Biochim. Biophys. Acta **1377,** R25-R44
https://doi.org/10.1016/S0304-419X(98)00003-1

Coskun O, Comlekci S (2013): The influence of pulsed electric field on hematological parameters in rat. Toxicol. Ind. Health **29,** 862-866
https://doi.org/10.1177/0748233712446724

Coskun Ö, Naziroglu M, Cömlekçi S, Özkorucuklu S, Elmas O (2011): Effects of 50 Hertz-1 mT magnetic field on action potential in isolated rat sciatic nerve. Toxicol. Ind. Health **27,** 127-132
https://doi.org/10.1177/0748233710381893

Daish C, Blanchard R, Fox K, Pivonka P, Pirogova E (2018): The application of pulsed electromagnetic fields (PEMFs) for bone fracture repair: Past and perspective findings. Ann. Biomed. Eng. **46,** 525-542
https://doi.org/10.1007/s10439-018-1982-1

Ellis RE, Yuan JY, Horvitz HR (1991): Mechanisms and functions of cell death. Ann. Rev. Cell Biol. **7,** 663-698
https://doi.org/10.1146/annurev.cb.07.110191.003311

Erkanli K, Kayalar N, Erkanli G, Ercan F, Sener G, Kirali K (2005): Melatonin protects against ischemia/reperfusion injury in skeletal muscle. J. Pineal Res. **39,** 238-242
https://doi.org/10.1111/j.1600-079X.2005.00240.x

Esper AM, Martin GS (2009): Extending international sepsis epidemiology: the impact of organ dysfunction. Crit. Care **13,** 120
https://doi.org/10.1186/cc7704

Flatscher J, Pavez Loriè E, Mittermayr R, Meznik P, Slezak P, Redl H, Slezak C (2023): Pulsed electromagnetic fields (PEMF)-physiological response and its potential in trauma treatment. Int. J. Mol. Sci. **24,** 11239
https://doi.org/10.3390/ijms241411239

Gessi S, Merighi S, Bencivenni S, Battistello E, Vincenzi F, Setti S, Cadossi M, Borea PA, Cadossi R, Varani K (2019): Pulsed electromagnetic field and relief of hypoxia-induced neuronal cell death: The signaling pathway. J. Cell. Physiol. **234,** 15089-15097
https://doi.org/10.1002/jcp.28149

Gevrek F, Gencel OS, Görgün S, Kara M, Katar M (2024): Evaluation of the aquaporin molecules characterization in the sperm cells of men from different aged. Turk. J. Med. Sci. **54,** 204-212
https://doi.org/10.55730/1300-0144.5781

Gevrek F, Yelli S, Gürgül S (2023): The impact of pulsed magnetic field on sepsis-induced liver tissue injury in rats. Gen. Physiol. Biophys. **42,** 539-549
https://doi.org/10.4149/gpb_2023026

Gul SS, Gurgul S, Uysal M, Erdemir F (2018): The protective effects of pulsed magnetic field and melatonin on testis torsion and detorsion induced rats indicated by scintigraphy, positron emission tomography/computed tomography and histopathological methods. Urology J. **15,** 387-396

Gustafsson AB, Gottlieb RA (2007): Bcl-2 family members and apoptosis, taken to heart. Am. J. Physiol. Cell Physiol. **292,** C45-C51
https://doi.org/10.1152/ajpcell.00229.2006

Habimana R, Choi I, Cho HJ, Kim D, Lee K, Jeong I (2020): Sepsis-induced cardiac dysfunction: a review of pathophysiology. Acute Crit. Care **35,** 57-66
https://doi.org/10.4266/acc.2020.00248

Haddad JJ (2007): The role of Bax/Bcl-2 and pro-caspase peptides in hypoxia/reperfusion-dependent regulation of MAPK(ERK): discordant proteomic effect of MAPK(p38). Protein Pept. Lett. **14,** 361-371
https://doi.org/10.2174/092986607780363925

Kang PM, Haunstetter A, Aoki H, Usheva A, Izumo S (2000): Morphological and molecular characterization of adult cardiomyocyte apoptosis during hypoxia and reoxygenation. Circ. Res. **87,** 118-125
https://doi.org/10.1161/01.RES.87.2.118

Kannan K, Jain SK (2000): Oxidative stress and apoptosis. Pathophysiology **7,** 153-163
https://doi.org/10.1016/S0928-4680(00)00053-5

Kirshenbaum LA, de Moissac D (1997): The bcl-2 gene product prevents programmed cell death of ventricular myocytes. Circulation **96,** 1580-1585
https://doi.org/10.1161/01.CIR.96.5.1580

Krijnen PA, Nijmeijer R, Meijer CJ, Visser CA, Hack CE, Niessen HW (2002): Apoptosis in myocardial ischaemia and infarction. J. Clin. Pathol. **55,** 801-811
https://doi.org/10.1136/jcp.55.11.801

Lee CG, Park C, Hwang S, Hong JE, Jo M, Eom M, Lee Y, Rhee KJ (2022): Pulsed electromagnetic field (PEMF) treatment reduces lipopolysaccharide-induced septic shock in mice. Int. J. Mol. Sci. **23,** 5661
https://doi.org/10.3390/ijms23105661

Mair J (1997): Cardiac troponin I and troponin T: Are enzymes still relevant as cardiac markers? Clin. Chim. Acta **257,** 99-115
https://doi.org/10.1016/S0009-8981(96)06436-4

Markov M (2015): XXIst century magnetotherapy. Electromagn. Biol. Med. **34,** 190-196
https://doi.org/10.3109/15368378.2015.1077338

Mattsson MO, Simkó M (2019): Emerging medical applications based on non-ionizing electromagnetic fields from 0 Hz to 10 THz. Med. Devices (Auckl.) **12,** 347-368
https://doi.org/10.2147/MDER.S214152

Mert T, Gunay I, Ocal I (2010): Neurobiological effects of pulsed magnetic field on diabetes-induced neuropathy. Bioelectromagnetics **31,** 39-47
https://doi.org/10.1002/bem.20524

Negahdary M, Namayandeh SM, Behjati-Ardekani M, Ghobadzadeh S, Dehghani H, Soltani MH (2015): The importance of the troponin biomarker in myocardial infarction. J. Biol. Today's World **5,** 1-12
https://doi.org/10.15412/J.JBTW.01050101

Oberholzer C, Oberholzer A, Clare-Salzler M, Moldawer LL (2001a): Apoptosis in sepsis: a new target for therapeutic exploration. FASEB J. **15,** 879-892
https://doi.org/10.1096/fsb2fj00058rev

Oberholzer C, Oberholzer A, Bahjat FR, Minter RM, Tannahill CL, Abouhamze A, LaFace D, Hutchins B, Clare-Salzler MJ, Moldawer LL (2001b): Targeted adenovirus-induced expression of IL-10 decreases thymic apoptosis and improves survival in murine sepsis Proc. Natl. Acad. Sci. USA **98,** 11503-11508
https://doi.org/10.1073/pnas.181338198

Oltvai ZN, Milliman CL, Korsmeyer SJ (1993): Bcl-2 heterodimerizes in vivo with a conserved homolog, Bax, that accelerates programmed cell death. Cell **74,** 609-619

https://doi.org/10.1016/0092-8674(93)90509-O
Pieber K, Schuhfried O, Fialka-Moser V (2007): Magnetfeldtherapie--Ergebnisse hinsichtlich evidence-based medicine (Pulsed electromagnetic fields (PEMF)--results in evidence-based medicine). Wien Med. Wochenschr. **157,** 34-36 (in German)
https://doi.org/10.1007/s10354-006-0369-3
Porter AG, Jänicke RU (1999): Emerging roles of caspase-3 in apoptosis. Cell Death Differ. **6,** 99-104
https://doi.org/10.1038/sj.cdd.4400476
Pu X, Storr SJ, Zhang Y, Rakha EA, Green AR, Ellis IO, Martin SG (2017): Caspase-3 and caspase-8 expression in breast cancer: caspase-3 is associated with survival. Apoptosis **22,** 357-368
https://doi.org/10.1007/s10495-016-1323-5
Qin AP, Zhang HL, Qin ZH (2008): Mechanisms of lysosomal proteases participating in cerebral ischemia-induced neuronal death. Neurosci. Bull. **24,** 117-123
https://doi.org/10.1007/s12264-008-0117-3
Radhakrishnan J, Ayoub IM, Gazmuri RJ (2009): Activation of caspase-3 may not contribute to postresuscitation myocardial dysfunction. Am. J. Physiol. Heart Circ. Physiol. **296,** H1164-H1174
https://doi.org/10.1152/ajpheart.00338.2008
Rosado MM, Simkó M, Mattsson MO, Pioli C (2018): Immune-modulating perspectives for low frequency electromagnetic fields in innate immunity. Front. Public Health **6,** 85
https://doi.org/10.3389/fpubh.2018.00085
Ross CL (2017): The use of electric, magnetic, and electromagnetic field for directed cell migration and adhesion in regenerative medicine. Biotechnol. Prog. **33,** 5-16
https://doi.org/10.1002/btpr.2371
Senol N, Kaya E, Coskun O, Aslankoc R, Comlekci S (2023): Evaluation of the effects of a 50 hz electric field on brain tissue by immunohistochemical method, and on blood tissue by biochemical, physiological and comet method. Appl. Sci. **13,** 3276-3288
https://doi.org/10.3390/app13053276
Şimşek T, Karakurt S, Gökçek-Saraç Ç (2022): Effect of pulsed electromagnetic field exposure on glutathione amount in human neuroblastoma cell line treated with high-dose hydrogen peroxide. SDUFASJS **17,** 146-154 (in Turkish)
https://doi.org/10.29233/sdufeffd.1029835
Soltani D, Samimi S, Vasheghani-Farahani A, Shariatpanahi SP, Abdolmaleki P, Madjid Ansari A (2023): Electromagnetic field therapy in cardiovascular diseases: A review of patents, clinically effective devices, and mechanism of therapeutic effects. Trends. Cardiovasc. Med. **33,** 72-78
https://doi.org/10.1016/j.tcm.2021.10.006
Sun Z, Shen L, Sun X, Tong G, Sun D, Han T, Yang G, Zhang J, Cao F, Yao L, et al. (2011): Variation of NDRG2 and c-Myc expression in rat heart during the acute stage of ischemia/reperfusion injury. Histochem. Cell Biol. **135,** 27-35
https://doi.org/10.1007/s00418-010-0776-9
Thornberry NA, Lazebnik Y (1998): Caspases: enemies within. Science **281,** 1312-1316
https://doi.org/10.1126/science.281.5381.1312
Tunca R, Erdogan HM, Sozmen M, Citil M, Devrim AK (2009): Evaluation of cardiac troponin I and inducible nitric oxide synthase expressions in lambs with white muscle disease. Turk. J. Vet. Anim. Sci. **33,** 53-59
https://doi.org/10.3906/vet-0710-6
van der Jagt OP, van der Linden JC, Waarsing JH, Verhaar JA, Weinans H (2012): Systemic treatment with pulsed electromagnetic fields do not affect bone microarchitecture in osteoporotic rats. Int. Orthop. **36,** 1501-1506
https://doi.org/10.1007/s00264-011-1471-8
van der Poll T, van de Veerdonk FL, Scicluna BP, Netea MG (2017): The immunopathology of sepsis and potential therapeutic targets. Nat. Rev. Immunol. **17,** 407-420
https://doi.org/10.1038/nri.2017.36
Vincenzi F, Ravani A, Pasquini S, Merighi S, Gessi S, Setti S, Cadossi R, Borea PA, Varani K (2017): Pulsed electromagnetic field exposure reduces hypoxia and inflammation damage in neuron-like and microglial cells. J. Cell. Physiol. **232,** 1200-1208
https://doi.org/10.1002/jcp.25606
Vulczak A, Catalão CHR, Freitas LAP, Rocha MJA (2019): HSP-target of therapeutic agents in sepsis treatment. Int. J. Mol. Sci. **20,** 4255
https://doi.org/10.3390/ijms20174255
Waldorff EI, Zhang N, Ryaby JT (2017): Pulsed electromagnetic field applications: A corporate perspective. J. Orthop. Translat. **9,** 60-68
https://doi.org/10.1016/j.jot.2017.02.006
Wang P, Liu J, Yang Y, Zhai M, Shao X, Yan Z, Zhang X, Wu Y, Cao L, Sui B, et al. (2017): Differential intensity-dependent effects of pulsed electromagnetic fields on RANKL-induced osteoclast formation, apoptosis, and bone resorbing ability in RAW264.7 cells. Bioelectromagnetics **38,** 602-612
https://doi.org/10.1002/bem.22070
Wang XY, Zhang F, Zhang C, Zheng LR, Yang J (2020): The biomarkers for acute myocardial infarction and heart failure. Biomed. Res. Int. **2020,** 2018035
https://doi.org/10.1155/2020/2018035
Yang L, Zhou D, Cao J, Shi F, Zeng J, Zhang S, Yan G, Chen Z, Chen B, Guo Y, et al. (2023): Revealing the biological mechanism of acupuncture in alleviating excessive inflammatory responses and organ damage in sepsis: a systematic review. Front. Immunol. **14,** 1242640
https://doi.org/10.3389/fimmu.2023.1242640
Zhai M, Jing D, Tong S, Wu Y, Wang P, Zeng Z, Shen G, Wang X, Xu Q, Luo E (2016): Pulsed electromagnetic fields promote in vitro osteoblastogenesis through a Wnt/β-catenin signaling-associated mechanism. Bioelectromagnetics **37,** 152-162
https://doi.org/10.1002/bem.21961
Zhang G, Dong D, Wan X, Zhang Y (2022): Cardiomyocyte death in sepsis: Mechanisms and regulation (Review). Mol. Med. Rep. **26,** 257
https://doi.org/10.3892/mmr.2022.12773
Zhang R, Gao X, Hu F, Chen Q, Lei Z, Yang Y, Tian J (2022): Myocardial protective effect of sivelestat sodium in rat models with sepsis-induced myocarditis. J. Thorac. Dis. **14,** 4003-4011
https://doi.org/10.21037/jtd-22-1309
Zhao Y, Cheng Q (2022): Exogenous H2S protects against septic cardiomyopathy by inhibiting autophagy through the AMPK/mTOR pathway. Contrast Media Mol. Imaging **2022,** 8464082

https://doi.org/10.1155/2022/8464082
Zhu L, Yu Y, Chua BH, Ho YS, Kuo TH (2001): Regulation of sodium-calcium exchange and mitochondrial energetics by Bcl-2 in the heart of transgenic mice. J. Mol. Cell. Cardiol. **33,** 2135-2144 https://doi.org/10.1006/jmcc.2001.1476

Received: January 3, 2024
Final version accepted: July 19, 2024